

Three-dimensional carpal kinematics of trotting horses

H. M. CLAYTON, D. SHA, J. A. STICK and D. R. MULLINEAUX

McPhail Equine Performance Center, College of Veterinary Medicine, Michigan State University, East Lansing, Michigan 48824, USA.

Keywords: horse; kinematics; helical angles; locomotion; carpus

Summary

Reasons for performing study: Descriptions of 3D kinematics assist in understanding joint function and dysfunction, and are an essential step toward 3D inverse dynamic analysis.

Objectives: To measure 3D carpal joint motion during trotting.

Methods: Three-dimensional trajectories of bone-fixed markers on the radius and third metacarpus of the right forelimb of 3 healthy horses were recorded at 120 Hz using a 6-camera analysis system. Joint kinematics were calculated in terms of helical angles between the 2 segments using a spatial attitude method.

Results: All horses showed carpal extension and internal rotation of the metacarpus relative to the radius as the carpus assumed the close-packed position. In late stance, the carpus began a cycle of flexion that continued through midswing, accompanied by a small cycle of internal rotation. The direction of abduction/adduction varied between horses. The predominant rotational movement was flexion/extension, which showed a range of motion of $15 \pm 6^\circ$ in stance and $76 \pm 13^\circ$ in swing.

Conclusions: Carpal motions were generally similar between horses with the exception of abduction/adduction.

Potential relevance: Knowledge of carpal joint motion should assist in understanding the pathogenesis of carpal injuries. However, it seems probable that real differences exist between individuals; therefore, further investigations of the effect of conformation on carpal motion should be performed in a much larger population of horses.

Introduction

The majority of equine kinematic studies have been performed in 2D in the sagittal plane (Drevemo *et al.* 1993; Holmström *et al.* 1994; Back *et al.* 1995; Clayton *et al.* 2000a). Sagittal plane carpal joint kinematics have been reported for the walk (Hodson *et al.* 2000) and trot (Back *et al.* 1995; Johnston *et al.* 1997; Lanovaz *et al.* 1999). The complex structure of the equine carpus, with multiple rows of bones and articulations, suggests the likelihood of motions other than flexion/extension in a sagittal plane. Indeed, abduction/adduction and axial rotations can be observed, especially in gaited breeds, such as the Peruvian Paso in which *termino*, outward rotation of the distal forelimb, is a feature of the gait. A study of 3D carpal rotations in Missouri Foxtrotters showed that the flat walk and the fox trot had similar profiles for flexion and extension, but adduction/abduction

and axial rotation showed greater differences between gaits (Nicodemus 2000). Questions to be addressed by 3D analysis in horses include determination of which are consistent within and between horses, which are normally related or coupled with each other, and which movements vary with conformation or gait.

A full 3D analysis describes relative motion between 2 limb segments in terms of rotations in 3 directions and linear displacements of the segments along the 3 axes of rotation. Unlike a multi planar 2D analysis, 3D analysis does not consider the segments to rotate around a joint centre. Instead, movements are described in terms of relative motion between 2 segments. Another difference is that in 2D analysis movements are expressed in a global coordinate system, whereas in 3D analysis, a local coordinate system that coincides with the anatomical axes of the bone is embedded within each segment, with angles and displacements being measured relative to these segmental coordinate systems. Rotational motion is measured in 3 directions between the corresponding axes of the 2 segments, with one segment being considered to be fixed and movements of the other segment being measured relative to the fixed segment. Linear displacements (or translations) describe relative motion between the centres of the coordinate systems of the 2 segments along the mediolateral, proximodistal and craniocaudal axes of the fixed segment. It is important to realise that most of the linear displacements between segments are a consequence of bone movement during rotation, rather than being due to sliding motion of the articular surfaces.

One of the problems inherent in kinematic analysis is that skin-based markers move relative to the underlying bones, which can give rise to large errors when bone movements are reconstructed from surface markers (Reinschmidt *et al.* 1997). Markers fixed to bones represent bone motion accurately and have been used to study limb kinematics in human subjects (Lafortune *et al.* 1992; Reinschmidt *et al.* 1997), and in horses to study 2D limb kinematics (van Weeren *et al.* 1988, 1990a,b, 1992) and 3D kinematics of the tarsus (Lanovaz *et al.* 2002) and the metacarpophalangeal joint (Chateau *et al.* 2004).

Knowledge of 3D kinematics of complex joints, such as the tarsus and carpus, may aid in understanding the pathogenesis of injury and lameness. Furthermore, descriptions of 3D kinematics are an essential step towards 3D inverse dynamic analysis. The aims of this study were to use bone-fixed markers and a spatial attitude method to characterise the 6 degrees of freedom of motion of the equine carpal joint in an anatomically relevant, bone-based coordinate system (BCS), and to compare the type and amount of movement within and between 3 subjects.

*Author to whom correspondence should be addressed.

[Paper received for publication 10.05.04; Accepted 04.10.04]

TABLE 1: Physical data for the 3 subjects and descriptive data (mean \pm s.d.) for 5 trotting trials of each subject

Subject	Height (cm)	Mass (kg)	Radius length (mm)	Metacarpus length (mm)	Average speed (m/sec)	Stride duration (msec)	Stance (% of stride)
Horse 1	149	450	363	129	3.12 \pm 0.20	737 \pm 27	41.4 \pm 1.3
Horse 2	153	485	382	146	2.96 \pm 0.08	703 \pm 11	45.3 \pm 1.1
Horse 3	144	364	369	161	3.18 \pm 0.21	723 \pm 21	44.5 \pm 1.3
Group mean	149 \pm 5	433 \pm 62	370 \pm 11	145 \pm 16	3.08 \pm 0.11	721 \pm 17	43.7 \pm 2.1

Materials and methods

Subjects

With approval of the Institute's Committee on Animal Use and Care, 3 sound horses (mean \pm s.d. mass 433 \pm 63 kg; height 1.47 \pm 0.06 m) were used in this study.

Bone-fixed markers

A detailed explanation of the procedure for rigid attachment of marker triads to the bones has been provided previously (Lanovaz *et al.* 2002). In summary, 4.75 mm diameter Steinmann pins were inserted percutaneously, under general anaesthesia, into the radius and third metacarpal bone of the right forelimb at sites where the bone is subcutaneous. The radial pin was located on the lateral side, proximal to the lateral styloid process. The metacarpal pin was placed on the dorsolateral aspect of the bone. Post operatively, phenylbutazone¹ was administered orally, and mepivacaine (Carbocaine-V)² was infiltrated around the site of pin insertion prior to data collection.

The next day, all subjects were judged subjectively to move willingly and normally during data collection.

Data collection and preprocessing

Subjects were prepared by attaching a triad of 25 mm diameter, spherical, reflective markers to each bone pin. In addition to the bone-fixed markers, reflective markers were attached to the skin (Fig 1) to define the local coordinate systems. In order to express the kinematics of the bones in a meaningful way, the coordinate systems for the radius and third metacarpus were based on the anatomy of the bones. Three easily palpable landmarks on each bone were chosen to define the bone-based coordinate system (BCS). Skin markers were attached overlying the following landmarks on the lateral side of the limb: the radial tuberosity (Rad_{prox}), lateral styloid process (Rad_{dist}), dorsal edge of the head of the fourth metacarpal bone (MC_{prox}) and third metacarpal condyle at the proximal attachment of the lateral collateral ligament of the metacarpophalangeal joint (MC_{dist}).

Subjects were placed in a normal standing position within the data collection volume and 4 additional markers were attached to the medial aspect of the limb to locate the third markers defining the BCS for the radius and third metacarpal bone. For the radius, the medial styloid process (Rad_{med}) was midway between markers V1 and V2 that projected on the cranial and caudal sides of the limb (Fig 1). For the third metacarpal bone, the dorsal edge of the head of the second metacarpal bone (MC_{med}) was midway between markers V3 and V4 that projected on the dorsal and palmar sides of the limb. The standing file was used during data processing to establish the local coordinate systems for the radius and metacarpus. After recording the standing file, markers on the medial side of the limb were removed.

Kinematic data of the standing horse were collected with both the bone marker triads and the skin markers on the lateral side of the limb in place. The radial and metacarpal BCS were established for the standing position using the kinematic data from the bony landmarks. From each BCS, a transformation matrix was developed and used to transform the locations of the triad markers in the standing position from the global coordinate system (GCS) to their corresponding BCS. Since the marker triads were fixed to the bone, the relationships between the marker triad orientations and their corresponding BCS did not change. For the trotting trials, the triad markers were tracked and a singular-value decomposition method (Söderkvist and Wedin 1993) was used to calculate the position and orientation of the BCS of the radius and metacarpal bone.

Data collection took place on a 40 m rubber-covered runway in which a 60 x 120 cm² force plate³ was embedded. Subjects were led in hand at the trot. Three-dimensional kinematic data were collected in the laboratory GCS using a 6-camera analysis system recording at 120 Hz with RealTime3.2 software⁴. A volume measuring 5 x 2 x 3 m was calibrated. In the configuration used for this study, the kinematic data collection system has an

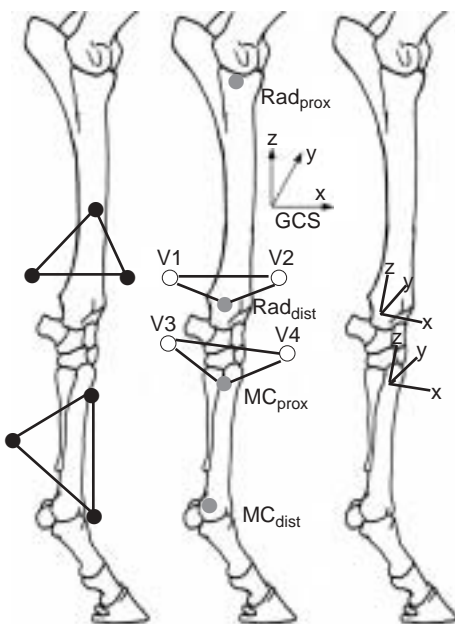


Fig 1: Configuration of markers used in kinematic calculations. Bone-fixed marker triads (●) were used to track the movements of the radial and metacarpal segments and to calculate carpal joint kinematics. Virtual markers (○ V1–4) and proximal and distal markers on the radial and metacarpal segments (●) were used to determine bone-based local coordinate systems. Note that the virtual markers appear higher than their actual position. x = cranial/caudal; y = medial/lateral; z = proximal/distal as shown on right.

TABLE 2: Range of carpal joint rotations and translations in 3 subjects, 5 strides per subject, and mean values for the group. Values are mean \pm s.d.

Kinematic variable	Stance phase				Swing phase			
	Horse 1	Horse 2	Horse 3	Group mean	Horse 1	Horse 2	Horse 3	Group mean
Flexion/extension (°)	9 \pm 3	16 \pm 3	21 \pm 4	15 \pm 6	89 \pm 3	64 \pm 2	77 \pm 1	76 \pm 13
Adduction/abduction (°)	4 \pm 0	5 \pm 1	6 \pm 1	5 \pm 1	11 \pm 2	8 \pm 1	19 \pm 1	13 \pm 6
Internal/external rotation (°)	2 \pm 1	5 \pm 2	4 \pm 0	4 \pm 1	9 \pm 0	5 \pm 1	18 \pm 2	11 \pm 7
Cranial/caudal translation (mm)	12 \pm 3	19 \pm 3	25 \pm 7	19 \pm 7	75 \pm 3	71 \pm 2	66 \pm 3	70 \pm 5
Medial/lateral translation (mm)	4 \pm 1	4 \pm 1	10 \pm 1	6 \pm 3	11 \pm 1	11 \pm 0	21 \pm 2	14 \pm 6
Proximal/distal translation (mm)	3 \pm 1	5 \pm 2	7 \pm 1	5 \pm 2	60 \pm 2	28 \pm 1	49 \pm 2	45 \pm 16

error on the order of 0.88 mm when measuring a known length (Lanovaz *et al.* 2002).

A successful trial consisted of a single stride of the right forelimb, starting with stance on the force plate, and with the force data being used to detect the onset and termination of right forelimb stance. Data were analysed using custom-written code in MATLAB⁵. Kinematic data from the trot trials were filtered using a fourth-order Butterworth filter with a cut-off frequency of 12 Hz. Lengths of data were normalised as 101 points for a full stride. The bone-fixed marker triads and the skin-based markers were tracked for each trial. At least 5 trials from each horse were recorded, with forward velocities being closely matched between subjects (Table 1).

Bone coordinate systems

For the radial BCS (Fig 1), a right-handed coordinate system was developed by first defining the flexion/extension axis (y) as the vector running from Rad_{dist} to Rad_{med}, which was midway between virtual markers V1 and V2. The adduction/abduction axis (x) of the radius was defined as a vector pointing cranially and perpendicular to the plane formed by the flexion/extension axis (y) and the vector running from Rad_{dist} to Rad_{prox}. Finally, the internal/external rotation axis (z) of the radius was defined as a vector pointing proximally along the long axis of the bone and perpendicular to the plane formed by the flexion/extension and adduction/abduction axes. The origin of the radial BCS was embedded in the bone midway between Rad_{dist} and Rad_{med}.

For the metacarpal BCS (Fig 1), a right-handed coordinate system was developed by first defining the flexion/extension axis (y) as the vector running from MC_{prox} to MC_{med}, which was midway between virtual markers V3 and V4. The adduction/abduction axis (x) of the metacarpus was defined as a vector pointing cranially and perpendicular to the plane formed by the flexion/extension axis (y) and the vector running from MC_{prox} to MC_{dist}. Finally, the internal/external rotation axis (z) of the metacarpus was defined as a vector pointing proximally along the long axis of the bone and perpendicular to the plane formed by the flexion/extension and adduction/abduction axes. The origin of the metacarpal BCS was embedded in the bone midway between MC_{prox} and MC_{med}.

Kinematic calculations

To calculate the kinematics of joints in the sense of anatomical position (Grood and Suntay 1983), the radial and metacarpal marker triads in the standing file were transformed from the GCS to the corresponding BCS defined above. The orientation matrices and displacement vectors were then calculated for the standing file and for each frame of trotting data using a singular value decomposition method (Söderkvist and Wedin 1993).

Relative angular motion between the radius and third metacarpal bone was expressed in terms of a spatial attitude vector (Woltring 1994). This method is based on the finite helical axis representation of relative motion, where the position and orientation of one body with respect to another at any given moment can be described as a scalar rotation around, and a linear displacement along, an axis between the bodies (Woltring *et al.* 1985). The spatial attitude vector is used to describe the relative angular orientations and is calculated by multiplying the scalar finite helical angle with the components of the unit vector describing the helical axis with respect to one of the bodies. This results in 3 orthogonal angular values that are expressed in terms of the coordinate axes of one of the bodies. The angular values are independent of the body they are referenced from, only the signs are different.

In this study, the spatial attitude vector was calculated with respect to the proximal segment of the joint as suggested by Woltring (1994), and the relative angular motions (helical angle changes) between the radial and metacarpal segments were calculated using a spatial attitude method (Spoor and Veldpaus 1980; Woltring 1994). The angular values can be thought of as though the radius is fixed and the third metacarpus is moving relative to it. Therefore, the flexion(+)/extension(-), adduction(+)/abduction(-) and internal(+)/external(-) rotation components of the attitude vector that describe the angular motion of the carpal joint are expressed in terms of the corresponding axes in the radius. Linear displacements between the centres of the radial and metacarpal coordinate systems were measured along the 3 axes; mediolateral motion was measured along the flexion/extension (y) axis, craniocaudal displacement along the abduction/adduction (x) axis, and proximodistal motion along the internal/external rotation (z) axis.

Data analysis

Five trials of each horse were analysed. The 3 rotations and 3 linear displacements were plotted separately for each horse and the shape of the curves was evaluated subjectively. The range of motion for each of the rotations and linear displacements was measured separately during stance and swing phases. Means \pm s.d. were calculated on a horse-by-horse basis and used to calculate the group mean and s.d. Visual evaluation of the graphs indicated the possibility of a relationship between flexion/extension and displacements in the proximal/distal direction and in the cranial/caudal direction. This was further investigated by plotting the rotation vs. the displacements and fitting a curve to the data points.

Results

Table 1 shows the physical data and stride variables for each subject. The average stride duration was 706 \pm 16 msec, with an average stance percentage of 43.5 \pm 2.4% of stride duration. The

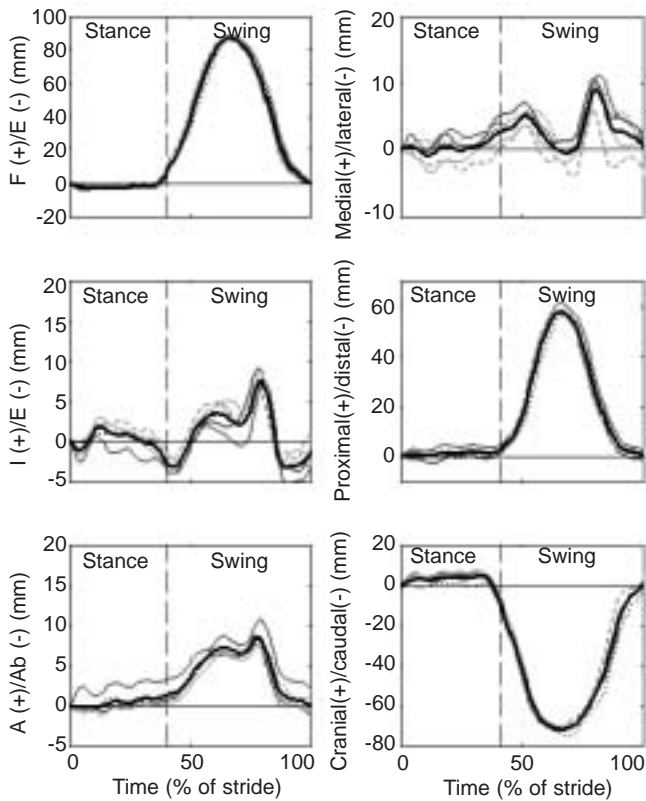


Fig 2: Carpal joint rotations (left) and translations (right) for Horse 1 during one stride at trot commencing at hoof contact. The mean trace is indicated by the heavy line. The dashed vertical line indicates lift-off. F = flexion; E = extension; I = internal; A = adduction; Ab = abduction.

ranges of motion were larger during swing than stance for all rotations and linear displacements (Table 2). The largest ranges of motion were for flexion/extension, cranial/caudal displacement and proximal/distal displacement.

Within each individual horse, the rotational and linear movements were quite consistent, with the greatest variation being shown by *Horse 1* (Fig 2). However, the shape and direction of adduction/abduction differed between horses (Fig 3). *Horses 1* and *3* had a cycle of adduction during swing, whereas *Horse 2* maintained a small amount of abduction throughout most of the stride, with greater stride-to-stride variability than the other horses. During stance, *Horse 3* showed lateral displacement of the metacarpus, whereas *Horses 1* and *2* showed a small amount of medial displacement. For the other rotations and linear displacements the patterns were similar between horses, but the magnitudes varied, especially for flexion/extension and proximal/distal displacement (Fig 3).

The angles at the start of stance (Table 3) indicate low variability between different strides of the same horse, and greater variability between horses. Differences between horses in range of flexion/extension during stance (Table 2) are primarily due to different amounts of carpal flexion at lift-off, rather than to differences in the amount of carpal flexion in the earlier part of stance, which was fairly similar in all subjects (Fig 3). Similarly, the range of cranial/caudal motion during stance included a variable amount of caudal displacement of the origin of the metacarpal BCS that was coupled with flexion of the joint at lift-off (Fig 3).

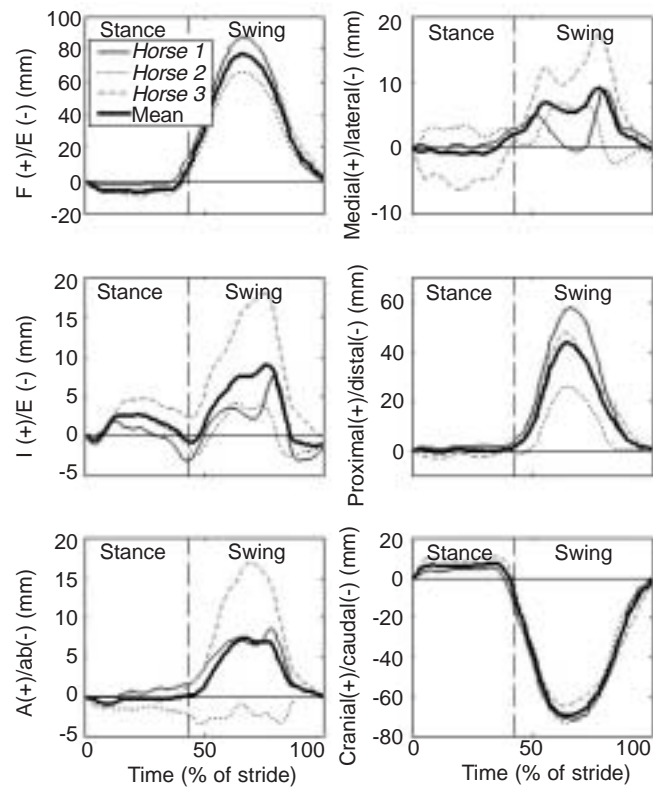


Fig 3: Carpal joint rotations (left) and linear displacements (right). The lines show mean values for individual horses and mean trace for the group of horses during one stride at trot commencing at hoof contact. The dashed vertical line indicates lift-off. Note different scales. See Figure 2 for explanation of abbreviations.

Consistent features of carpal kinematics were that, in early stance, the carpus extended and rotated inward, and the origin of the metacarpal BCS moved cranially relative to the radius (Fig 3). This position was maintained until late stance. Just before lift-off, the carpus began to flex and rotate externally. The flexion continued into midswing, resulting in proximal and caudal displacement of the origin of the metacarpal BCS. At the same time, there was a small amount of internal rotation and medial displacement of the metacarpal BCS.

The curves for flexion/extension vs. the proximal/distal and cranial/caudal displacements showed a small amount of hysteresis around the time of peak flexion (Fig 4) and the curves were therefore analysed in 2 parts; from the start of swing to maximal carpal flexion, and from maximal flexion to the end of swing. In each case the relationship was primarily linear, but a 2nd order polynomial improved the fit and resulted in an $r^2 > 0.99$ in all cases (equations listed in Fig 4).

Discussion

The shape of the flexion/extension curve and the range of movement in this study are similar to those reported in 2D studies of the carpus (Back *et al.* 1995), even though the flexion/extension axis of the joint defined by the BCS was not necessarily perpendicular to the sagittal plane of the horse. This was expected, since misalignments of the flexion/extension axis have little effect on the rotational movements for joints where flexion/extension dominates (Ramakrishnan and Kadaba 1991).

TABLE 3: Repeatability of joint orientation at the start of the stride

Kinematic variables	Group mean \pm s.d.	
	at start of stride (all 3 horses)	Mean of s.d. for individual horses at start of stride
Flexion(+)/extension(-) ($^{\circ}$)	3.4 \pm 2.6	1.1
Adduction(+)/abduction(-) ($^{\circ}$)	-6.9 \pm 12.6	1.1
Internal(+)/external(-) ($^{\circ}$)	-7.8 \pm 6.9	1.2
Cranial(+)/caudal(-) trans (mm)	-5.8 \pm 11.1	1.7
Medial(+)/lateral(-) trans (mm)	5.2 \pm 9.3	1.1
Proximal(+)/distal(-) trans (mm)	-96.2 \pm 9.8	1.6

trans = translation.

When motion at a joint is dominated by one type of rotation, in this case flexion/extension, errors may arise as a consequence of slight misalignments of the BCS. Establishment of the BCS is based on the location of skin markers in the standing file. In this study, errors in setting up the BCS were reduced by using easily-palpable bony landmarks and having the same researcher apply the markers on all horses. In spite of these precautions, there may have been slight differences between horses in BCS orientation. Even small differences in orientation of the BCS can result in rotations other than flexion/extension being measured when none exist, or can obscure the presence of rotations that are actually present (Piazza and Cavanagh 1999). This could account for interhorse differences in abduction/adduction. On the other hand, if the angular differences between subjects are real, they may reflect conformational variation. This should be investigated further in a larger number of subjects with a range of carpal conformations.

In early stance, the carpus compresses into the so-called 'close-packed' position in which the articular surfaces are fully congruent. This study has shown that, as it assumes the close-packed position, the carpus undergoes extension and internal rotation, combined with a little cranial displacement of the metacarpus similar to the screw-home mechanism described in the human knee. The slightly extended position of the carpus during stance, while being supported by a flexor torque (Clayton *et al.* 2000b), allows the forelimb to act as a rigid strut as the body mass is propelled forward over the grounded limb. The forces associated with carpal loading during stance could play a role in the aetiology of carpal fractures. Higher speeds are likely to engender larger compressive and shear forces, increasing the risk of injury. It is hypothesised that the tendency of the carpus to translate medially or laterally in an individual horse may play a role in the development of carpal injuries, although data from the trot cannot necessarily be extrapolated to other gaits.

In the swing phase, the carpus flexes to raise the hoof clear of the ground as the limb is protracted, then extends as the limb is prepared for the start of the next stance phase. Carpal flexion in early swing was accompanied by a little internal rotation. As a consequence of the hinge-like motion of the antebrachio-carpal and intercarpal joints, the origin of the BCS in the proximal metacarpus moved caudally (~ 7 cm) and proximally (~ 4 cm) relative to the origin of the radial BCS. *Horse 1* showed more carpal flexion ($>80^{\circ}$) than the other horses and also had the largest caudal displacement.

The 2nd order polynomial was a very good fit for both the ascending and descending arms of the curves in Figure 4. Although the value of the x^2 component of the polynomial equation was small, it made an important contribution to the fit. Hysteresis in the curves may represent sliding motions at the

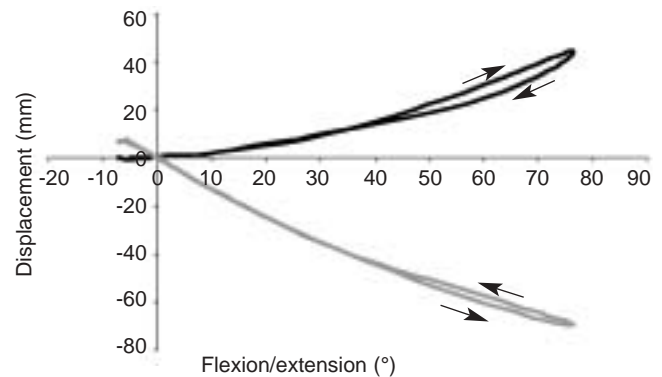


Fig 4: Relationships between flexion/extension and proximal/distal translation (black line) and cranial/caudal translation (grey line).

Direction of curves is indicated by arrows. The equations were as follows:

Flexion/extension vs. proximal/distal translation:

$$\text{Ascending curve: } y = 0.0055x^2 + 0.1788x - 0.6584, r^2 = 0.9993$$

$$\text{Descending curve: } y = 0.006x^2 + 0.0711x + 0.8577, r^2 = 0.9943$$

Flexion/extension vs. cranial/caudal translation:

$$\text{Descending curve: } y = 0.0052x^2 - 1.3089x - 0.5254, r^2 = 0.9998$$

$$\text{Ascending curve: } y = 0.0052x^2 - 1.2809x - 0.4739, r^2 = 0.9991$$

articular surfaces. Consequently, as the carpus extended in the second half of swing, the origin of the metacarpal BCS was slightly more cranial and distal relative to the origin of the radial BCS than during the preceding flexion. This might have been the result of laxity in the carpal ligaments of the flexed joint allowing a widening and forward sliding of the articular surface of the metacarpus relative to the radius.

Sagittal plane motion of the carpus during swing has been shown to be driven by inertia; power generated at the elbow drives the movements of the more distal joints with the amount of motion being controlled passively by the surrounding soft tissues (Lanovaz *et al.* 1999). If carpal movements, other than flexion/extension, are also driven inertially, swing phase kinematics might be affected by laxity of the stabilising soft tissues, which could contribute to differences between individuals in medial/lateral displacement.

Movement of surface markers attached to the skin may not represent the actual movement of the underlying bone because of soft tissue deformation (van Weeren *et al.* 1992). To avoid this problem, bone-fixed markers can be used for direct measurement of skeletal motion. This technique provides the most accurate approach for determining bone movements (Lanovaz *et al.* 2002). Bone-fixed markers have been used in man, with none of the subjects reporting pain or substantial discomfort during the experiments (Reinschmidt *et al.* 1997). In horses, bone-fixed markers have been used to study many limb joints (van Weeren *et al.* 1988, 1990a,b, 1992; Lanovaz *et al.* 2002; Chateau *et al.* 2004). The subjects in this study appeared to move quite normally within 24 h after pin placement. However, the invasiveness of the procedure argues against using more subjects than is absolutely necessary. In this study, only 3 subjects were used. Even so, there was considerable interhorse variability in some of the movements, particularly abduction/adduction and medial/lateral displacement. The possibility that these were due to differences in orientation of the BCS has been discussed earlier. However, it seems probable that there are some real differences between individuals resulting, for example, in the variation in flight path of the distal limb that results in the hoof arcing medially or laterally during swing.

Further investigations of the effect of conformation on carpal motion should be performed in a much larger population of horses.

In summary, this study presents full 3D kinematics with 3 degrees of freedom in rotation and 3 degrees of freedom in linear displacement (translation), describing relative motion between the radial and metacarpal segments of 3 horses at trot. The results indicate similarity in patterns between horses, with the exceptions of adduction/abduction and medial/lateral displacements. Differences between horses may arise from inconsistencies in orientation of the BCS or they may be a result of conformational variation. The largest magnitude of rotation was flexion during swing, which is correlated with proximal and caudal displacement of the origin of the metacarpal BCS relative to the origin of the radial BCS as a consequence of the hinge-like action of the antebrachiocarpal and intercarpal joints.

Acknowledgement

The authors acknowledge the financial support of the McPhail endowment.

Manufacturers' addresses

¹Schering-Plough, Kenilworth, New Jersey, USA

²Pharmacia and Upjohn Company, Kalamazoo, Michigan, USA

³Motion Analysis Corporation, Santa Rosa, California, USA.

⁴AMTI, Watertown, Massachusetts, USA.

⁵MathWorks Inc, Natick, Massachusetts, USA

References

- Back, W., Schamhardt, H.C., Savelberg, H.H.C.M., van den Bogert, A.J., Bruin, G., Hartman, W. and Barneveld, A. (1995) How the horse moves: significance of graphical representations of equine forelimb kinematics. *Equine vet. J.* **27**, 31-38.
- Chateau, H., Degueurce, C. and Denoix, J.-M. (2004) Evaluation of three-dimensional kinematics of the distal portion of the forelimb in horses walking in a straight line. *Am. J. vet. Res.* **65**, 447-455.
- Clayton, H.M., Schamhardt, H.C., Willemsen, M.A., Lanovaz, J.L. and Colborne, G.R. (2000a) Kinematics and ground reaction forces in horses with superficial digital flexor tendinitis. *Am. J. vet. Res.* **61**, 191-196.
- Clayton, H.M., Schamhardt, H.C., Willemsen, M.A., Lanovaz, J.L. and Colborne, G.R. (2000b) Net joint moments and joint powers in horses with superficial digital flexor tendinitis. *Am. J. vet. Res.* **61**, 197-201.
- Drevemo, S., Roepstorff, L., Kallings, P. and Johnston, C.J. (1993) Application of TrackEye, in Equine locomotion research. *Acta Anat.* **146**, 137-140.
- Good, E.W. and Suntay, W.J. (1983) A joint coordinate system for the clinical description of three-dimensional motions: applications to the knee. *J. Biomech. Eng.* **105**, 136-144.
- Hodson, E.F., Clayton, H.M. and Lanovaz, J.L. (2000) The forelimb in walking horses: I. Kinematics and ground reaction forces. *Equine vet. J.* **32**, 287-294.
- Holmström, M., Fredricson, I. and Drevemo, S. (1994) Biokinematic analysis of the Swedish Warmblood riding horse at the trot. *Equine vet. J.* **26**, 235-240.
- Johnston, C., Drevemo, S. and Roepstorff, L. (1997) Kinematics and kinetics of the carpus. *Equine vet. J., Suppl.* **23**, 84-88.
- Lafortune, M.A., Cavanagh, P.R., Sommer, H.J. III and Kalenak, A. (1992) Three-dimensional kinematics of the human knee during walking. *J. Biomech.* **25**, 347-357.
- Lanovaz, J.L., Clayton, H.M., Colborne, G.R. and Schamhardt, H.C. (1999) Forelimb kinematics and net joint moments during the swing phase of the trot. *Equine vet. J., Suppl.* **30**, 235-239.
- Lanovaz, J.L., Khumsap, S., Clayton, H.M., Stick, J.A. and Brown, J. (2002) Three-dimensional kinematics of the tarsal joint at the trot. *Equine vet. J., Suppl.* **34**, 308-313.
- Nicodemus, M.C. (2000) *Quantification of the Locomotion of Gaited Horses*. PhD Thesis, Michigan State University, Michigan.
- Piazza, S.J. and Cavanagh, P.R. (1999) Measurement of the screw-home motion of the knee is sensitive to errors in axis alignment. *Abstr. Am. Soc. Biomech.* **23**, <http://asb-biomech.org/onlineabs/abstracts99/111/>
- Ramakrishnan, H.K. and Kadaba, M.P. (1991) On the estimation of joint kinematics during gait. *J. Biomech.* **24**, 969-997.
- Reinschmidt, C., van den Bogert, A.J., Murphy, N., Lundberg, A. and Nigg, B.M. (1997) Tibiocalcaneal motion during running- measured with external and bone markers. *Clin. Biomech.* **12**, 8-16.
- Söderkvist, I. and Wedin, P.A. (1993) Determining the movements of the skeleton using well-configured markers. *J. Biomech.* **26**, 1473-1477.
- Spoor, C.W. and Veldpaus, F.E. (1980) Rigid body motion calculated from spatial coordinates of markers. *J. Biomech.* **13**, 391-393.
- van Weeren, P. R., van den Bogert, A.J. and Barneveld, A. (1988) Quantification of skin displacement near the carpal, tarsal and fetlock joints of the walking horse. *Equine vet. J.* **20**, 203-208.
- van Weeren, P.R., van den Bogert, A.J. and Barneveld, A. (1990a) Quantification of skin displacement in the proximal parts of the limbs of the walking horse. *Equine vet. J., Suppl.* **9**, 110-119.
- van Weeren, P.R., van den Bogert, A.J. and Barneveld, A. (1990b) A quantitative analysis of skin displacement in the trotting horse. *Equine vet. J., Suppl.* **9**, 101-109.
- van Weeren, P.R., van den Bogert, A.J. and Barneveld, A. (1992) Correction models for skin displacement in equine kinematic gait analysis. *J. equine vet. Sci.* **12**, 178-192.
- Woltring, H.J. (1994) 3-D attitude representation of human joints: a standardization proposal. *J. Biomech.* **27**, 1399-1414.
- Woltring, H.J., Huiskes, R., de Lange, A. and Veldpaus, F.E. (1985) Finite centroid and helical axis estimation from noisy landmark measurements in the study of human joint kinematics. *J. Biomech.* **18**, 379-389.